3.2. The enhancement of the activation of HSCs with VEGF-treated LSEC CM via TGF-β

We investigated the molecular mechanism through which VEGF induces hepatic fibrosis in mice using primary cell culture systems. As assessed by the lack of an increase in the α-SMA levels (a marker of activated HSCs), VEGF did not directly activate isolated primary HSCs after 5 days of treatment at 100 and 200 ng/ml, concentrations that are nearly equivalent to the blood concentration of VEGF in in vivo experiments (Fig. 2A). VEGF also did not affect the mRNA expressions of TGF-β1, PLK, and uPAR (Fig. 2B). VEGF enhanced latent TGF-β1 concentration (1.1-fold at 200 ng/ml VEGF) in LSEC CM (Fig. 2C) and mRNA expressions of TGF-β1 (2.4-fold at 200 ng/ml VEGF), PLK (2.1-fold at 200 ng/ml VEGF), and uPAR (1.8-fold at 200 ng/ml VEGF) in LSECs (Fig. 2D). HSCs were activated via incubation with recombinant TGF-β1 (100 pg/ml) and LSEC CM, the latter of which was blocked by incubation with neutralizing antibodies against TGF-β1 (Fig. 2E).

3.3. Latent TGF-β secreted from LSECs is activated by PLK on the surface of HSCs

Given the ELISA and bioassay results, we found that primary LSECs secreted only 2.5% of TGF-β in the active form during 24 h incubation (Fig. 2C), and that the active TGF-β concentrations in LSEC CM were slightly higher than those in the control medium (DMEM containing 2% FBS) (Fig. 2C). To investigate whether latent TGF-β present in LSEC CM was activated by PLK as we previously showed [9], we cultured primary HSCs with LSEC CM with or without PI-PLC, which cleaves the glycophosphatidylinositol anchor, re-

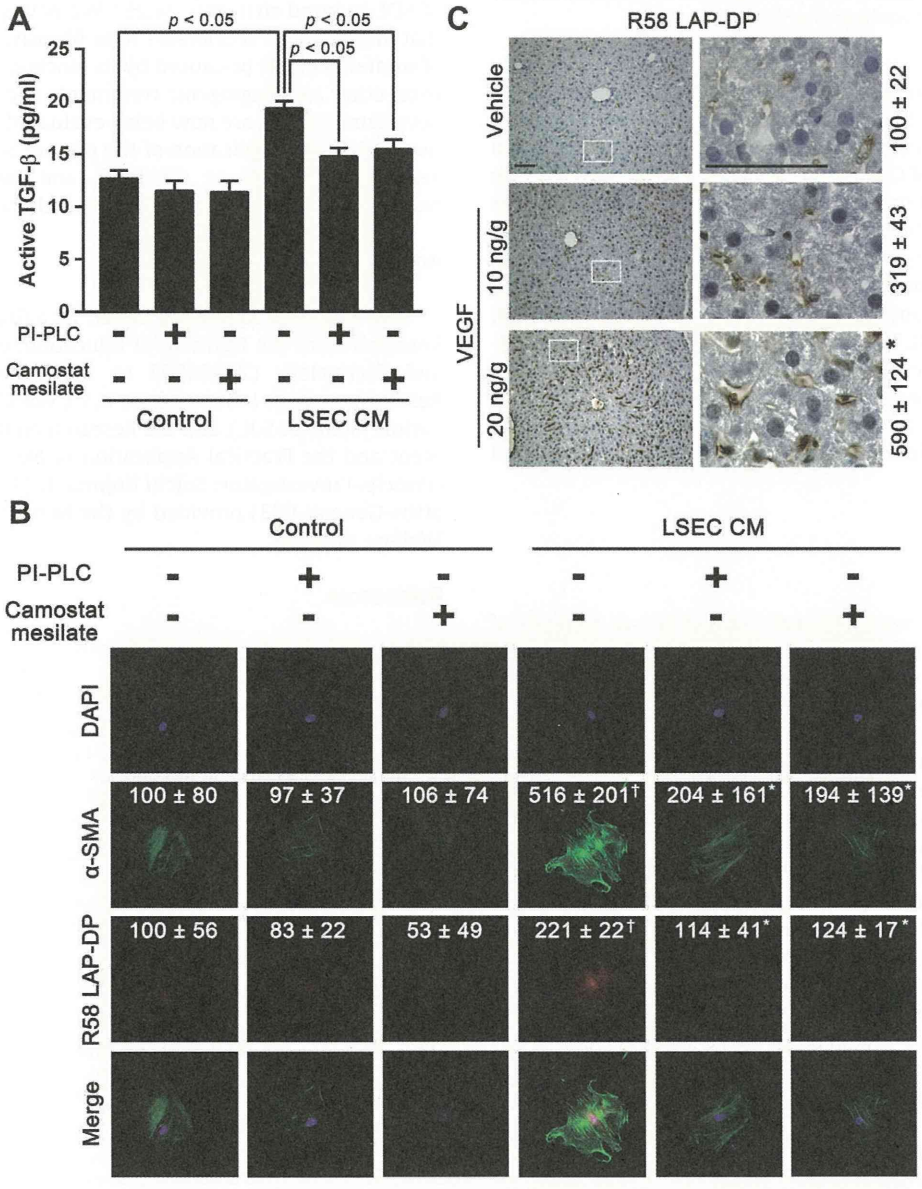

Fig. 3. Latent TGF-β derived from LSECs was activated on the surface of hepatic stellate cells through PLK in in vitro and in vivo. Primary HSCs were incubated with 2% FBS DMEM or LSEC CM in the presence or absence of PI-PLC (0.5 U/mL) or camostat mesilate (500 μM) for 5 days. (A) Active TGF-β1 levels in the media were measured using the luciferase assay in $(CAGA)_9$-Luc CCL64 cells. Data are shown as the means ± SD. (B) Cells were fixed and stained with α-SMA and R58 LAP-DPs as described in the Section 2. The relative fluorescence intensities (% of untreated control cells) are shown as the means ± SD. (C) The liver sections harvested from the VEGF-injected mice were stained with anti-R58 LAP-DPs antibody, as described in the Section 2. The right panels show higher magnifications of the corresponding white squares in the left panels. Scale bars, 100 μm. Positive areas (%) were quantitated and shown as the means ± SD ($n = 3$). $^{\dagger}p < 0.05$ compared with untreated control cells, $^{*}p < 0.05$ compared with LSEC CM-treated control cells.

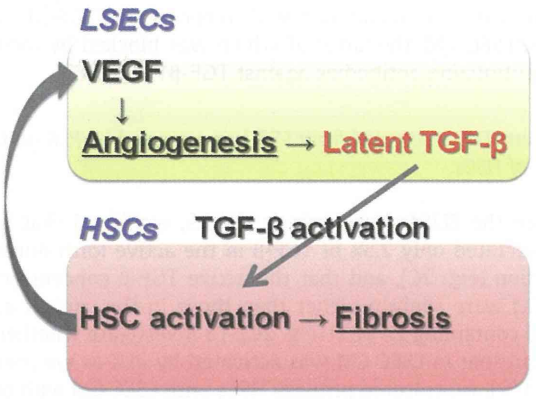

Fig. 4. The scheme of the molecular mechanism through which angiogenesis promotes fibrosis in the liver. Increased neovessels provided with latent TGF-β, which PLK activates on the surface of HSCs and stimulates the activation of HSCs. Therefore, angiogenesis might accelerate liver fibrosis.

leases uPAR and its associated with PLK from the cell surface, or with or without camostat mesilate, a serine protease inhibitor. Both these treatments resulted in a reduction in the concentration of active TGF-β in the LSEC CM (Fig. 3A). LSEC CM failed to activate the HSCs that had been incubated with either PI-PLC or camostat mesilate (Fig. 3B). The R58 LAP-DP levels, a footprint of PLK-dependent TGF-β activation [9], were reduced via either PI-PLC or camostat mesilate. VEGF did not affect R58 LAP-DPs expression (Relative fluorescent intensity: Control 100 ± 56; VEGF 100 ng/ml 112 ± 30; VEGF 200 ng/ml 99 ± 48). To confirm whether PLK-dependent activation might be increased along with neovessel formation in vivo, the liver sections harvested from the VEGF-administered mice were stained with anti-R58 LAP-DPs antibody. As expected, the R58-positive area was increased with VEGF injection by 5.9-fold (Fig. 3C).

4. Discussion

In the present study, we addressed a role of ECs as a source of latent TGF-β, the precursor of the most fibrogenic cytokine TGF-β. We provided in vitro evidence that LSEC CM promotes the activation of quiescent HSCs via the provision of latent TGF-β and in vivo evidence that much more severe fibrosis was induced in the livers of mice that received VEGF (Fig. 4). These data suggest that HSC activation is promoted not only via changes in the extracellular matrix, inflammatory cytokines, and oxidative stress but also secondarily via pathological angiogenesis.

We documented that TGF-β, which is secreted from LSECs as a latent form and activated on the surface of mainly HSCs rather than LSECs (compare Figs. 3A and 2C), mediates enhancement in liver fibrosis, although the expressions of PLK and uPAR increased 2-fold in VEGF-treated LSECs (Fig. 2D). Several groups have reported that VEGF enhanced the expression of urokinase-type plasminogen activator and its receptor uPAR in both bovine microvascular endothelial cells and human umbilical vein endothelial cells [19], enabling them matrix degradation and cell invasion [20], and that bradykinin production via the PLK-dependent cleavage of high molecular weight kininogen promotes angiogenesis via the upregulation of basic fibroblast growth factor [21]. In our study, increased PLK in LSECs might interact with HSCs and promote TGF-β activation on the surface of HSCs. At the same time, increased uPAR and PLK in LSECs also might contribute to angiogenesis. We showed that VEGF increased the levels of hepatic CD31 by 3.6-fold and R58 LAP-DPs by 5.9-fold in mice and that VEGF enhanced latent TGF-β production and TGF-β1 mRNA expression in primary LSECs. These data also suggest that LSECs serve as the source of TGF-β for liver fibrosis.

Yoshiji et al. demonstrated that VEGF receptor expression increased in HSCs along with the development of fibrosis and that a neutralizing anti-VEGF receptor antibody attenuated both angiogenesis and fibrogenesis in the liver [22], using activated HSCs, whereas we used quiescent HSCs. The result in Fig. 1 suggests that VEGF promotes the growth of LSECs, which appears to serve as a source of latent TGF-β, thereby increasing the hepatic levels of TGF-β1, due to the increased number of LSECs in the early stages of liver fibrosis (Fig. 4). Eventually, HSCs were activated and began to express the VEGF receptor, respond to VEGF, and transition to a more activated state. However, we cannot rule out the involvement of other soluble factors, such as PDGF, which is also produced from LSECs and stimulates HSC activation [11,23].

Sorafenib, a multikinase inhibitor recently approved to treat unresectable hepatocellular carcinoma, was beneficial in a model of BDL-induced cirrhosis [24,25]. We have provided here evidence that angiogenesis accelerates liver fibrosis. The anti-fibrotic effect of sorafenib might be caused by its blocking of angiogenesis. Moreover, other anti-angiogenic treatments such as vatalanib [26] and bevacizumab [27], are now being evaluated in clinical cancer treatment trials. An implication of the current study is that anti-angiogenic agents such as vatalanib and bevacizumab might be beneficial for anti-fibrotic therapy in addition to sorafenib.

Acknowledgments

This work was supported in part by a Grant-in-Aid for Scientific Research from the Ministry of Education, Culture, Sports, Science and Technology (23390202 to S.K.), Grants for Collaborative Researchers from Industries (to K.S.), the Uehara Memorial Foundation, Japan (to S.K.), and the Research on the Innovative Development and the Practical Application of New Drugs for Hepatitis B (Principal investigator: Soichi Kojima; H24-B Drug Discovery-Hepatitis-General-003) provided by the Ministry of Health, Labor and Welfare of Japan.

References

[1] S.L. Friedman, Mechanisms of hepatic fibrogenesis, Gastroenterology 134 (2008) 1655–1669.
[2] R. Bataller, D.A. Brenner, Liver fibrosis, J. Clin. Invest. 115 (2005) 209–218.
[3] N.C. Henderson, T.D. Arnold, Y. Katamura, M.M. Giacomini, J.D. Rodriguez, J.H. McCarty, A. Pellicoro, E. Raschperger, C. Betsholtz, P.G. Ruminski, D.W. Griggs, M.J. Prinsen, J.J. Maher, J.P. Iredale, A. Lacy-Hulbert, R.H. Adams, D. Sheppard, Targeting of αv integrin identifies a core molecular pathway that regulates fibrosis in several organs, Nat. Med. 19 (2013) 1617–1624.
[4] S.L. Friedman, Hepatic stellate cells: protean, multifunctional, and enigmatic cells of the liver, Physiol. Rev. 88 (2008) 125–172.
[5] H. Tsukamoto, Cytokine regulation of hepatic stellate cells in liver fibrosis, Alcohol. Clin. Exp. Res. 23 (1999) 911–916.
[6] F.R. Weiner, M.A. Giambrone, M.J. Czaja, A. Shah, G. Annoni, S. Takahashi, M. Eghbali, M.A. Zern, Ito-cell gene expression and collagen regulation, Hepatology 11 (1990) 111–117.
[7] M. Matsuoka, N.T. Pham, H. Tsukamoto, Differential effects of interleukin-1α, tumor necrosis factor α, and transforming growth factor β1 on cell proliferation and collagen formation by cultured fat-storing cells, Liver 9 (1989) 71–78.
[8] S.B. Jakowlew, J.E. Mead, D. Danielpour, J. Wu, A.B. Roberts, N. Fausto, Transforming growth factor-β (TGF-β) isoforms in rat liver regeneration: messenger RNA expression and activation of latent TGF-β, Cell Regul. 2 (1991) 535–548.
[9] K. Akita, M. Okuno, M. Enya, S. Imai, H. Moriwaki, N. Kawada, Y. Suzuki, S. Kojima, Impaired liver regeneration in mice by lipopolysaccharide via TNF-α/kallikrein-mediated activation of latent TGF-β, Gastroenterology 123 (2002) 352–364.
[10] S. Kojima, Detection of hepatic fibrogenesis targeting proteolytic TGF-β activation reaction, Hepatology (2008) 917A.
[11] D. Thabut, V. Shah, Intrahepatic angiogenesis and sinusoidal remodeling in chronic liver disease: new targets for the treatment of portal hypertension?, J Hepatol. 53 (2010) 976–980.
[12] B.S. Ding, D.J. Nolan, J.M. Butler, D. James, A.O. Babazadeh, Z. Rosenwaks, V. Mittal, H. Kobayashi, K. Shido, D. Lyden, T.N. Sato, S.Y. Rabbany, S. Rafii,

Inductive angiocrine signals from sinusoidal endothelium are required for liver regeneration, Nature 468 (2010) 310–315.
[13] M. Fernandez, D. Semela, J. Bruix, I. Colle, M. Pinzani, J. Bosch, Angiogenesis in liver disease, J. Hepatol. 50 (2009) 604–620.
[14] H. Sahin, E. Borkham-Kamphorst, C. Kuppe, M.M. Zaldivar, C. Grouls, M. Al-samman, A. Nellen, P. Schmitz, D. Heinrichs, M.L. Berres, D. Doleschel, D. Scholten, R. Weiskirchen, M.J. Moeller, F. Kiessling, C. Trautwein, H.E. Wasmuth, Chemokine Cxcl9 attenuates liver fibrosis-associated angiogenesis in mice, Hepatology 55 (2012) 1610–1619.
[15] G.K. Reddy, C.S. Enwemeka, A simplified method for the analysis of hydroxyproline in biological tissues, Clin. Biochem. 29 (1996) 225–229.
[16] S. Kitazume, R. Imamaki, K. Ogawa, Y. Komi, S. Futakawa, S. Kojima, Y. Hashimoto, J.D. Marth, J.C. Paulson, N. Taniguchi, α2,6-sialic acid on platelet endothelial cell adhesion molecule (PECAM) regulates its homophilic interactions and downstream antiapoptotic signaling, J. Biol. Chem. 285 (2010) 6515–6521.
[17] P.K. Datta, H.L. Moses, STRAP and Smad7 synergize in the inhibition of transforming growth factor β signaling, Mol. Cell. Biol. 20 (2000) 3157–3167.
[18] K. Sakata, M. Hara, T. Terada, N. Watanabe, D. Takaya, S. Yaguchi, T. Matsumoto, T. Matsuura, M. Shirouzu, S. Yokoyama, T. Yamaguchi, K. Miyazawa, H. Aizaki, T. Suzuki, T. Wakita, M. Imoto, S. Kojima, HCV NS3 protease enhances liver fibrosis via binding to and activating TGF-β type I receptor, Sci. Rep. 3 (2013) 3243.
[19] S.J. Mandriota, G. Seghezzi, J.D. Vassalli, N. Ferrara, S. Wasi, R. Mazzieri, P. Mignatti, M.S. Pepper, Vascular endothelial growth factor increases urokinase receptor expression in vascular endothelial cells, J. Biol. Chem. 270 (1995) 9709–9716.
[20] J.M. Breuss, P. Uhrin, VEGF-initiated angiogenesis and the uPA/uPAR system, Cell Adh. Migr. 6 (2012) 535–615.
[21] R.W. Colman, Regulation of angiogenesis by the kallikrein–kinin system, Curr. Pharm. Des. 12 (2006) 2599–2607.
[22] H. Yoshiji, S. Kuriyama, J. Yoshii, Y. Ikenaka, R. Noguchi, D.J. Hicklin, Y. Wu, K. Yanase, T. Namisaki, M. Yamazaki, H. Tsujinoue, H. Imazu, T. Masaki, H. Fukui, Vascular endothelial growth factor and receptor interaction is a prerequisite for murine hepatic fibrogenesis, Gut 52 (2003) 1347–1354.
[23] J.S. Lee, D. Semela, J. Iredale, V.H. Shah, Sinusoidal remodeling and angiogenesis: a new function for the liver-specific pericyte?, Hepatology 45 (2007) 817–825
[24] D. Thabut, C. Routray, G. Lomberk, U. Shergill, K. Glaser, R. Huebert, L. Patel, T. Masyuk, B. Blechacz, A. Vercnocke, E. Ritman, R. Ehman, R. Urrutia, V. Shah, Complementary vascular and matrix regulatory pathways underlie the beneficial mechanism of action of sorafenib in liver fibrosis, Hepatology 54 (2011) 573–585.
[25] M. Mejias, E. Garcia-Pras, C. Tiani, R. Miquel, J. Bosch, M. Fernandez, Beneficial effects of sorafenib on splanchnic, intrahepatic, and portocollateral circulations in portal hypertensive and cirrhotic rats, Hepatology 49 (2009) 1245–1256.
[26] J.M. Wood, G. Bold, E. Buchdunger, R. Cozens, S. Ferrari, J. Frei, F. Hofmann, J. Mestan, H. Mett, T. O'Reilly, E. Persohn, J. Rosel, C. Schnell, D. Stover, A. Theuer, H. Towbin, F. Wenger, K. Woods-Cook, A. Menrad, G. Siemeister, M. Schirner, K.H. Thierauch, M.R. Schneider, J. Drevs, G. Martiny-Baron, F. Totzke, PTK787/ZK 222584, a novel and potent inhibitor of vascular endothelial growth factor receptor tyrosine kinases, impairs vascular endothelial growth factor-induced responses and tumor growth after oral administration, Cancer Res. 60 (2000) 2178–2189.
[27] N. Ferrara, K.J. Hillan, H.P. Gerber, W. Novotny, Discovery and development of bevacizumab, an anti-VEGF antibody for treating cancer, Nat. Rev. Drug. Discovery 3 (2004) 391–400.

Hepatology Research

Hepatology Research 2013; **43**: 276–288 doi: 10.1111/j.1872-034X.2012.01062.x

Original Article

Altered expression and function of hepatic natural killer T cells in obese and diabetic KK-A^y mice

Hisafumi Yamagata,[1] Kenichi Ikejima,[1] Kazuyoshi Takeda,[2] Tomonori Aoyama,[1] Kazuyoshi Kon,[1] Ko Okumura[2] and Sumio Watanabe[1]

Departments of [1]Gastroenterology and [2]Immunology, Juntendo University Graduate School of Medicine, Tokyo, Japan

Aim: To evaluate the role of natural killer (NK)T cells in the pathogenesis of non-alcoholic steatohepatitis (NASH), here we investigated the expression and function of hepatic NKT cells in KK-A^y mice, an animal model of metabolic syndrome.

Methods: Male, 8-week-old KK-A^y and C57Bl/6 mice were fed a high-fat (HF) diet for 4 weeks. Some mice were given daily intragastric injections of pioglitazone for 5 days prior to or after dietary treatment.

Results: In untreated KK-A^y mice, the percentages of NKT cells in liver mononucleolar cells were nearly one-third of those in C57Bl/6 controls. Elevations in interleukin (IL)-4 and interferon (IFN)-γ mRNA in the liver after a single injection of α-galactosylceramide (GalCer) were blunted in KK-A^y mice largely. Percentages of NKT cells, as well as GalCer-induced increases in IL-4 mRNA, were blunted significantly in both strains after HF diet feeding for 4 weeks. Interestingly, KK-A^y mice pretreated with pioglitazone showed significant increases in NKT cell proportion, and GalCer-induced increases in IL-4 and IFN-γ mRNA were also enhanced by pioglitazone. In KK-A^y mice, the percentages of annexin V positive NKT cells were nearly 2.5-fold higher than those in C57Bl/6 controls; however, pioglitazone decreased annexin V positive cells significantly. Moreover, pioglitazone increased NKT cell fraction in KK-A^y mice even after HF diet feeding.

Conclusion: KK-A^y mice exhibit proportional and functional alterations in hepatic NKT cells in close relation with the development of steatohepatitis, and it is postulated that pioglitazone improves steatohepatitis in part through restoration of hepatic NKT cells.

Key words: adipokines, innate immunity, metabolic syndrome, natural killer T cells, non-alcoholic steatohepatitis, pioglitazone

INTRODUCTION

NON-ALCOHOLIC FATTY LIVER disease (NAFLD), which is the liver manifestation of metabolic syndrome, has become the most common cause of chronic liver disease in industrialized countries worldwide.[1–3] NAFLD contains a spectrum of liver pathology ranging from simple hepatic steatosis to non-alcoholic steatohepatitis (NASH), which demonstrates progressive diseases such as advanced liver fibrosis and hepatocellular carcinoma.[1–3] It is widely accepted that insulin resistance is the common and profound pathophysiological basis of NAFLD as well as metabolic syndrome;[4] however, the mechanism by which only a portion of NAFLD patients develop progressive liver disease has not been well elucidated. Various environmental and nutritional factors as well as genetic susceptibilities appear to be involved in progression of NASH. Especially, genetic and epigenetic factors related to oxidative stress, innate immunity and tissue repairing responses most likely regulate the severity of metabolic abnormalities, hepatic inflammation and fibrogenesis. Among these, it is postulated that adipokines, a group of cytokines produced exclusively from adipose tissue (i.e. leptin, adiponectin, resistin, plasminogen activator inhibitor-1), modulate both metabolic balance and progression of hepatic disorder.[4]

Recent studies have suggested that alteration in the innate immune system is involved in the pathogenesis of NASH.[5,6] It is well known that the liver contains a variety of immune cells, with considerable proportion of natural killer (NK)T-cell fraction.[7] NKT cells are a heterogeneous subset of lymphocytes expressing both

Correspondence: Dr Kenichi Ikejima, Department of Gastroenterology, Juntendo University Graduate School of Medicine, 2-1-1 Hongo, Bunkyo-ku, Tokyo 113-8421, Japan. Email: ikejima@juntendo.ac.jp
Received 26 March 2012; revision 5 June 2012; accepted 14 June 2012.

NK and T-cell surface markers.[8,9] Classical (type I) NKT cells express an invariant T-cell receptor (TCR) containing the Vα14-Jα18 chain in mice, whereas non-classical (type II) NKT cells express diverse TCR.[8] NKT cells recognize a glycolipid antigen presented by CD1d, one of the major histocompatibility complex molecules, on antigen-presenting cells such as dendritic cells and macrophages.[8,10] Several studies suggested that NKT cells modulate hepatic inflammation and fibrogenesis;[11–15] however, the precise role of these cells in liver pathophysiology is still controversial. It has been reported that hepatic NKT cells are depleted in *ob/ob* mice which develop severe hepatic steatosis essentially caused by genetic disruption of leptin (*ob*) gene,[16,17] suggesting that leptin is an important regulator of innate immune responses in the liver.

Clinically relevant animal models are required to investigate the pathophysiology and experimental therapeutics of NAFLD/NASH. KK-A^y mice are a cross-strain of diabetic KK mice[18] and lethal yellow (A^y) mice, which carry mutation of the agouti(a) gene in mouse chromosome 2.[19] KK-A^y mice develop maturity-onset obesity, dyslipidemia and insulin resistance, in part because of the antagonism of melanocortin receptor-4 by ectopic expression of the agouti protein.[19] Importantly, these mice present hyperleptinemia and leptin resistance without defects in the leptin receptor (*ObR*) gene, and the expression of adiponectin is conversely downregulated.[20,21] The phenotype of KK-A^y mice, including altered adipokine expression, quite resembles that of most common patients of metabolic syndrome in humans, indicating potential usefulness of this strain as a model of metabolic syndrome-related NASH. Indeed, KK-A^y mice are more susceptible to experimental steatohepatitis induced by a methionine- and choline-deficient diet.[21] It has also been reported that KK-A^y mice are vulnerable to acute liver injury caused by lipopolysaccharide and galactosamine,[20] and acetaminophen.[22] In addition, we have reported recently that hepatic regeneration after partial hepatectomy is impaired in KK-A^y mice.[23] These observations have suggested that KK-A^y mice bear functional abnormalities in the innate immune system; however, the phenotypic characteristics of innate immunity, especially in terms of NKT cells in the liver, have not been explored extensively.

In the present study, we therefore investigated the changes in hepatic NKT cells in obese and diabetic KK-A^y mice. Further, we evaluated the effect of pioglitazone, a thiazolidinedione derivative (TZD), which improves insulin resistance through actions as a peroxisome proliferator-activated receptor (PPAR)-γ agonist, on expression and functional alteration in the NKT-cell subset in these animals.

METHODS

Animal experiments and dietary treatment

MALE KK-A^y AND C57Bl/6 mice 7 weeks after birth were obtained from CLEA Japan (Tokyo, Japan). Mice were housed in air-conditioned specific pathogen-free animal quarters with lighting from 08.00–21.00 hours, and given unrestricted access to a standard lab chow and water for 1 week prior to experiments. All animals received humane care in compliance with the experimental protocol approved by the Committee of Laboratory Animals according to institutional guidelines. C57Bl/6 mice were used as non-obese and non-diabetic controls. Some KK-A^y mice were treated with 25 mg/kg pioglitazone (a generous gift from Takeda Pharmaceutical, Tokyo, Japan) or vehicle by intragastric injection once daily for 5 days prior to or after dietary treatment. Mice were fed a high-fat (HF) diet which contained 56.7% of fat calories (HFD32; CLEA Japan; Table 1) or a control diet with 10% of fat calorie ad libitum for 4 weeks. This HF diet contains 32% total fat content, and the percentages of saturated, monounsaturated and polyunsaturated fatty acid in total fatty acid are 22.3%, 66.5% and 10.4%, respectively. Some mice were given a single peritoneal injection of α-galactosylceramide (GalCer, a generous gift from Kirin Breweries, Tokyo, Japan), a specific ligand for NKT-cell-specific TCR, and killed during the time course up to

Table 1 Components of high-fat diet (HFD32)

Ingredients (%)	High-fat diet (HFD32)	Control diet
Milk casein	24.5	17.5
Egg white powder	5.0	3.6
L-cystein	0.43	0.3
Tallow powder	15.88	1.95
Safflower oil	20.0	2.45
Microcrystalline cellulose	5.5	4.0
Maltodextrin	8.25	2.0
Lactose	6.928	2.3
Sucrose	6.75	–
Caster sugar	–	10.0
AIN93 vitamin mixture	1.4	1.0
AIN93G mineral mixture	5.0	3.5
Choline bitartrate	0.36	0.25
Tert-butylhydroquinone	0.002	0.0014
Corn starch	–	51.1486

24 h. Mice were killed by exsanguination from the inferior vena cava, and serum and liver samples were kept frozen at −80 °C until assayed.

Histopathological evaluation

For histological evaluation, liver specimens were fixed in buffered formalin for hematoxylin–eosin (HE) staining. To evaluate granulocyte infiltration, double staining for α-naphthyl acetate esterase and naphthol AS-D chloroacetate esterase was performed using a kit (Sigma Diagnostics, St Louis, MO, USA) according to the manufacturer's instruction. Specimens were observed and photographed using a microscope equipped with a digital imaging system (Leica DM 2000, Leica Microsystems, Wetzlar, Germany).

Measurement of serum aminotransferases and enzyme-linked immunoassay (ELISA)

Serum alanine aminotransferase levels were measured spectrophotometrically by a standard enzymatic method using a commercial kit (KAINOS Laboratories, Tokyo, Japan). Serum leptin and adiponectin levels were determined using ELISA kits (leptin, Seikagaku, Tokyo, Japan; adiponectin, Otsuka Pharmaceutical, Tokyo, Japan) according to the manufacturer's instruction.

Isolation of liver mononuclear cells and fluorescence-activated cell sorting (FACS) analysis

Under deep ether anesthesia, mice were killed by exsanguinations through the subclavian artery and vein, and the liver was harvested. The liver was passed through a stainless steel mesh and suspended in Hank's balanced salt solution. After one washing, the cells were resuspended in 30% Percoll containing 100 U/mL heparin, and centrifuged at 960 *g* for 15 min at room temperature. The pellet was resuspended in red blood cell lysis solution (155 mmol/L Na_4Cl, 10 mmol/L $KHCO_3$, 1 mmol/L ethylenediamine tetraacetic acid, 170 mol/L Tris, pH 7.3), and washed twice in 5% fetal bovine serum–Hank's balanced salt solution.

Surface phenotype of the NKT cells was characterized by two-color flow cytometry (FACS). Briefly, 1×10^6 cells were first pre-incubated with anti-CD16/32 (2.4G2) monoclonal antibody to avoid the non-specific binding of antibodies to FcγR. Then, the cells were incubated with fluorescein isothiocyanate (FITC)-conjugated anti-CD3ε monoclonal antibody (145-2C111) and phycoerythrin (PE)-conjugated anti-NK1.1 (PK136) monoclonal antibody (BD Pharmingen, San Jose, CA, USA). For detection of apoptosis, cells were stained with an Annexin V-PE Apoptosis Detection kit I (BD Pharmingen). After washing with phosphate-buffered saline (PBS), the stained cells were analyzed using FACS Calibur and CellQuest software (Becton Dickinson Bioscience, San Jose, CA, USA).

RNA preparation and real-time reverse transcription polymerase chain reaction (RT–PCR)

Total liver RNA was prepared from frozen tissue samples using an Illustra RNAspin Mini RNA Isolation kit (GE Healthcare, Buckinghamshire, UK). The concentration and purity of isolated RNA were determined by measuring optical density at 260 and 280 nm. Further, the integrity of RNA was verified by electrophoresis on formaldehyde denaturing agarose gels.

For real-time RT–PCR, total RNA (1 μg) were reverse transcribed using Moloney murine leukemia virus transcriptase (Super-Script II; Invitrogen, Carlsbad, CA, USA) and an oligo dT (12–18) primer (Invitrogen) at 42 °C for 1 h. Obtained cDNA (1 μg) was amplified using SYBR Premix Ex TaqTM (Takara Bio, Tokyo, Japan) and specific primers as appropriate. Primer sets were as follows: interleukin (IL)-4 (GenBank accession no.: NM_021283), forward, 5′-TCT CGA ATG TAC CAG GAG CCA TAT C-3′, reverse, 5′-AGC ACC TTG GAA GCC CTA CAG A-3′, yielding a 183-bp product; interferon (IFN)-γ (GenBank accession no.: NM_008337), forward, 5′-CGG CAC AGT CAT TGA AAG CCT A-3′, reverse, 5′-GTT GCT GAT GGC CTG ATT GTC-3′, yielding a 199-bp product; and glyceraldehyde 3-phosphate dehydrogenase (GAPDH) (GenBank accession no.: NM_001001303), forward, 5′-TGT GTC CGT CGT GGA TCT GA-3′, reverse, 5′-TTG CTG TTG AAG TCG CAG GAG-3′, yielding a 150-bp product. After a 10-s activation period at 95 °C, 40 cycles of 95 °C for 5 s and 60 °C for 31 s, followed by the final cycle of 95 °C for 15 s, 60 °C for 1 min and 95 °C for 15 s, were performed using an ABI PRISM 7700 Sequence Detection System (PE Applied Biosystems, Foster City, CA, USA), and the threshold cycle (C_T) values were obtained.

Statistical analysis

Data were expressed as means ± standard error of the mean. Statistical differences between means were determined using ANOVA on ranks followed by a post-hoc test (Student–Newman–Keuls all pairwise comparison procedures). $P < 0.05$ was selected before the study to reflect significance.

RESULTS

Hepatic NKT cells are depleted in KK-A^y mice before dietary treatment

WE FIRST EVALUATED the percentages of hepatic NKT-cell fraction in KK-A^y mice without dietary treatment using FACS analysis. Male KK-A^y mice 8 weeks after birth showed very mild hepatic steatosis with trivial inflammatory infiltration in hepatic lobules, as compared to C57Bl/6 mice as controls (Fig. 1a). In the control C57Bl/6 mice, the percentages of CD3- and NK1.1-double positive cells in the liver mononuclear cells were 27% before dietary treatment, whereas the values were only 9.9% in KK-A^y mice (Fig. 1b,c). These cell populations were disappeared 24 h after a single i.p. injection of GalCer in both strains, confirming that these populations are GalCer-sensitive NKT cells. We further checked the proportion of NKT cells in the liver and thymus in younger mice. The proportion of hepatic NKT cells in KK-A^y and C57Bl/6 mice at 4-week-old were almost the same, the values being 15.6 ± 2.4% and 15.7 ± 0.8%, respectively. In addition, NKT cells in thymus in these strains were 1.5 ± 0.5% and 1.5 ± 0.3%, respectively, where no significant difference were observed, indicating that NKT-cell maturation in thymus is not impaired in KK-A^y mice. Taken together, these findings suggest that depletion of NKT cells in KK-A^y mice is an acquired response.

To evaluate the response of hepatic NKT cells in these mice, we next gave a single injection of GalCer to these mice, and mRNA levels of IL-4 and IFN-γ, the two major NKT-cell-derived cytokines, were quantified by real-time RT–PCR (Fig. 1d,e). As expected, IL-4 mRNA in the liver was increased transiently after injection of GalCer in C57Bl/6 mice; however, the peak levels at 3 h in KK-A^y mice reached only one-sixth of values in C57Bl/6 mice (Fig. 1d). Similarly, IFN-γ mRNA peaked 12 h after injection of GalCer, whereas the levels in KK-A^y mice being one-fifth of those in C57Bl/6 mice (Fig. 1e). Collectively, these data indicated that the response of hepatic NKT cells to GalCer was markedly blunted in KK-A^y mice even before developing severe steatohepatitis.

HF diet induces more severe steatohepatitis in KK-A^y mice

Next, we evaluated the development of HF diet-induced steatohepatitis in KK-A^y mice. The control C57Bl/6 mice showed very mild hepatic steatosis even after HF diet feeding for 4 weeks as expected, whereas KK-A^y mice exhibited extremely severe steatosis following the same dietary treatment (Fig. 2a). Indeed, hepatic triglyceride content was markedly increased in KK-A^y mice fed a HF diet (Fig. 2B), confirming that KK-A^y mice develop more severe hepatic steatosis. Serum alanine aminotransferase levels were increased by HF diet feeding in both strains; however, the levels were much higher in KK-A^y mice than in C57Bl/6 mice (Fig. 2c). Further, we counted infiltrated granulocytes in the liver specimens by esterase staining. Granulocyte accumulation was significantly higher in KK-A^y mice fed a HF diet (Fig. 2d), indicating that HF diet feeding for 4 weeks induced more severe steatohepatitis in KK-A^y mice.

In terms of expression of adipokines, KK-A^y mice demonstrated overt hyperleptinemia and hypoadiponecitinemia even before dietary treatment as expected (Fig. 2e,f). In C57Bl/6 mice, serum leptin levels were not changed following 4-week feeding with HF diet. Serum adiponectin levels were decreased in these mice by HF diet feeding significantly. In contrast, HF diet feeding for 4 weeks enhanced both increases in serum leptin levels and decreases in serum adiponectin levels in KK-A^y mice.

HF diet decreases hepatic NKT-cell fraction in both C57Bl/6 and KK-A^y mice

Next, we evaluated the changes in NKT-cell fraction following HF diet feeding in both strains of mice (Fig. 3a,b). C57Bl/6 controls showed age-related mild increases in NKT-cell fraction, whereas HF diet feeding for 4 weeks decreased percentages of NKT cells to 18.1% (Fig. 3a). KK-A^y mice fed a HF diet showed extended decreases in NKT cell fraction as low as 8.3% (Fig. 3b).

Figure 3(c,d) demonstrate GalCer-induced increases in IL-4 and IFN-γ mRNA levels in HF diet-fed mice, respectively. GalCer-induced increases in IL-4 mRNA were blunted in C57Bl/6 mice fed a HF diet (Fig. 3c). In contrast, elevation in IFN-γ mRNA following injection of GalCer was not decreased in C57Bl/6 mice fed a HF diet (Fig. 3d). In KK-A^y mice, peak inductions of both IL-4 and IFN-γ were blunted by HF diet feeding (Fig. 3c,d).

Pioglitazone restores hepatic NKT cells in KK-A^y mice

Because insulin resistance is one of the important characteristics of KK-A^y mice, we next tested whether pioglitazone, an insulin sensitizer, affects hepatic NKT fraction in these mice. To test this, we first evaluated the effect of pioglitazone in 8-week-old KK-A^y mice before dietary treatment. Interestingly, KK-A^y mice pretreated with pioglitazone for 5 days showed significant

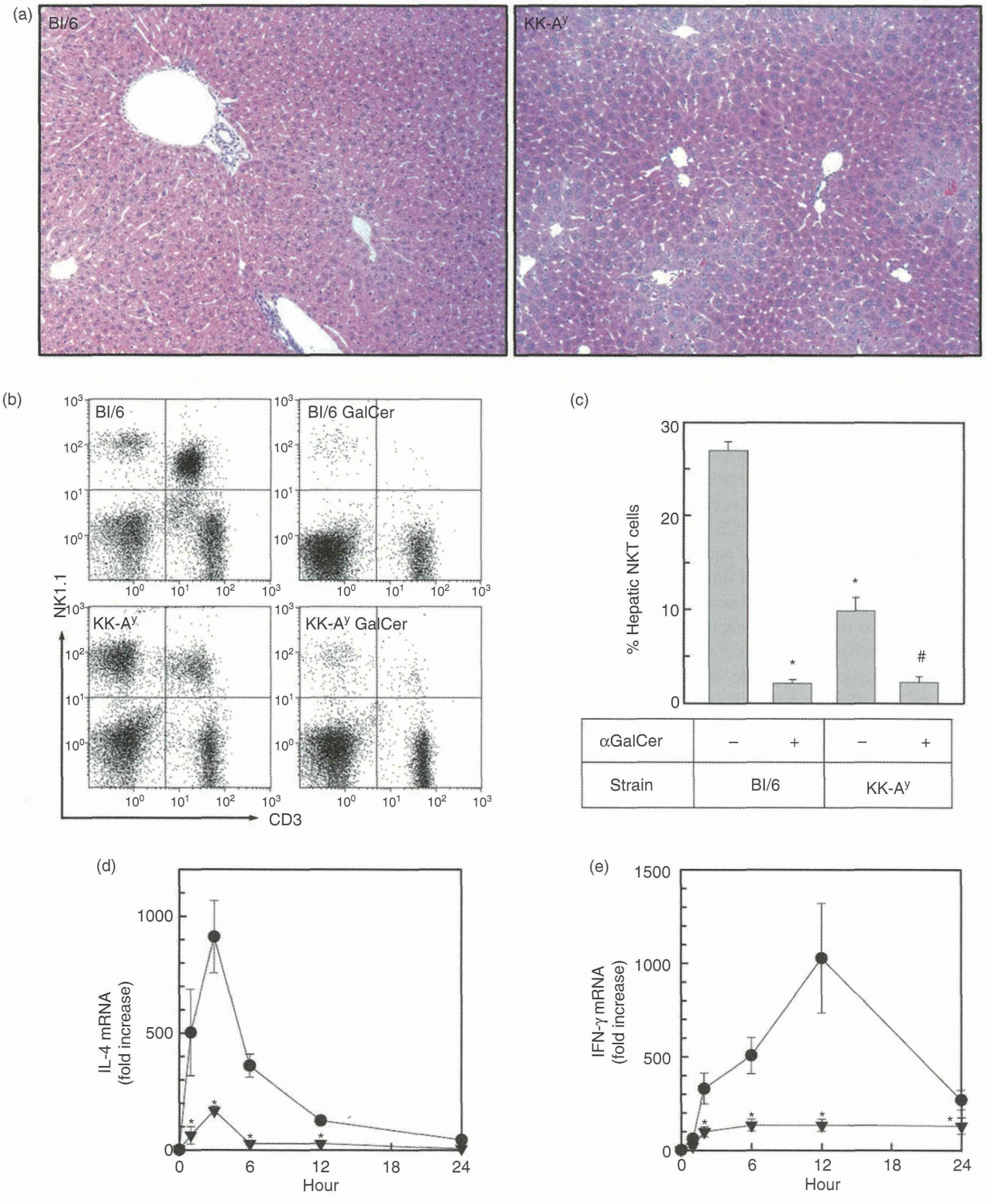

Figure 1 Expression of hepatic NKT cells in KK-A^y mice before dietary treatment. Representative photomicrographs of liver histology from 8-week-old male C57Bl/6 mice (a; left panel) and KK-A^y mice (a; right panel) are shown (hematoxylin–eosin, original magnification ×100). Hepatic NKT-cell fraction in each strain was detected by fluorescence-activated cell sorting analysis (b). CD3 and NK1.1 dual positive NKT cells are sequestered in the upper right quarter. Representative plots from untreated C57Bl/6 (b; left upper panel), Bl/6 given GalCer 24 h prior to harvest (b; right upper panel), untreated KK-A^y (b; left lower panel) and KK-A^y given GalCer (b; lower right panel) are shown. The average percentages of hepatic NKT cells are plotted (c; $n = 5$, mean ± SEM, $^*P < 0.05$ vs Bl/6 controls, $\#P < 0.05$ vs KK-A^y controls, by ANOVA on ranks and Student–Newman–Keuls post-hoc test). Steady state mRNA levels of IL-4 and IFN-γ in the liver following a single injection of GalCer in both strains were measured by real time reverse transcription polymerase chain reaction. Average values of fold increase over control C57Bl/6 levels for IL-4 (d) and IFN-γ (e) in C57Bl/6 (closed circle) and KK-A^y mice (closed triangle) are plotted ($n = 5$, mean ± SEM, $^*P < 0.05$ vs Bl/6 in each time point by ANOVA on ranks and Student–Newman–Keuls post-hoc test). GalCer, α-galactosylceramide; IFN, interferon; IL, interleukin; NKT cells, natural killer T cells; SEM, standard error of the mean.

elevation in NKT-cell proportion to the values reaching 18.3% (Fig. 4a,b). Further, GalCer-induced increases in IL-4 and IFN-γ mRNA were also enhanced in KK-A^y mice given pioglitazone (Fig. 4c,d).

Next, we analyzed apoptotic cell death in hepatic NKT cells by detecting annexin V expression (Fig. 5). In KK-A^y mice, annexin V positive NKT cells were increased nearly 2.7-fold higher than those in C57Bl/6 controls, whereas annexin V positive cells were significantly decreased in mice given pioglitazone for 5 days.

Moreover, HF diet-induced severe hepatic steatosis in KK-A^y mice was reversed largely by subsequent pioglitazone treatment for 5 days (Fig. 6a). Indeed, pioglitazone decreased hepatic triglyceride contents to nearly half values of HF diet-fed KK-A^y mice (Fig. 6b). As shown in Figure 6(c), pioglitazone treatment also increased NKT-cell fraction in KK-A^y mice fed a HF diet. Finally, pioglitazone significantly potentiated GalCer-induced increases in IL-4 and IFN-γ mRNA in the liver in KK-A^y mice fed a HF diet, the levels being 3.7- and 2.1-fold as compared to the values without pioglitazone, respectively ($P < 0.05$).

DISCUSSION

HERE, WE DEMONSTRATED that hepatic NKT cells are depleted in KK-A^y mice, which develop remarkable steatohepatitis following long-term feeding with HF diet (Fig. 2). This proportional changes in the NKT-cell population in the liver appear to be accompanied by functional abnormalities, because KK-A^y mice showed poor NKT-cell-derived cytokine responses in the liver following a single injection of GalCer, a synthetic ligand of NKT-cell-specific TCR (Fig. 1d,e). Importantly, the proportion of NKT cells is decreased in untreated KK-A^y mice 8 weeks after birth (Fig. 1), when these mice present very mild hepatic steatosis with trivial hepatic inflammation, indicating that NKT-cell depletion precedes development of severe hepatic steatohepatitis following HF diet-feeding. Further, feeding with a HF diet causes extended decreases in hepatic NKT cells in KK-A^y mice, while the same dietary treatment also decreases NKT-cell fraction in C57Bl/6 mice, which is coincident with a previous report by Li *et al.*[24] It is therefore hypothesized that hepatic NKT cells play a regulatory role in progression of steatohepatitis.

In the present study, we demonstrated that hepatic NKT cells are progressively depleted through induction of apoptosis (Fig. 5), suggesting that constitutive activation of NKT cells, which in turn elicits apoptotic cell death, occurs during the development of steatohepatitis. Emerging attention has been paid to the link between obesity, insulin resistance and alteration in gut bacterial flora.[25,26] Increased permeability of the gut mucosal barrier allows the entry of bacterial substances such as lipopolysaccharide to the portal blood flow, which participates in the pathogenesis of steatohepatitis.[27–30] It is therefore hypothesized that gut microbiota-derived glycolipid antigens would play a certain role in constitutive activation of NKT cells, which elicits production of T-helper (Th)2 cytokines, thus leading to the functional alteration in hepatic macrophages. These microenvironmental changes in the hepatic innate immune system are most likely involved in the metabolic abnormalities, inflammation and fibrogenesis in the liver. Indeed, emerging lines of evidence suggest that hepatic NKT cells are involved in hepatic fibrogenesis.[11–14] We have demonstrated recently that thioacetamide-induced hepatic inflammation and subsequent fibrogenesis are markedly ameliorated in CD1d knockout mice, which lack NKT cells systemically, suggesting that NKT cells promote inflammatory and profibrogenic responses in the liver.[15] Moreover, NKT cells are likely to prevent hepatocarcinogenesis based on steatohepatitis. Collec-

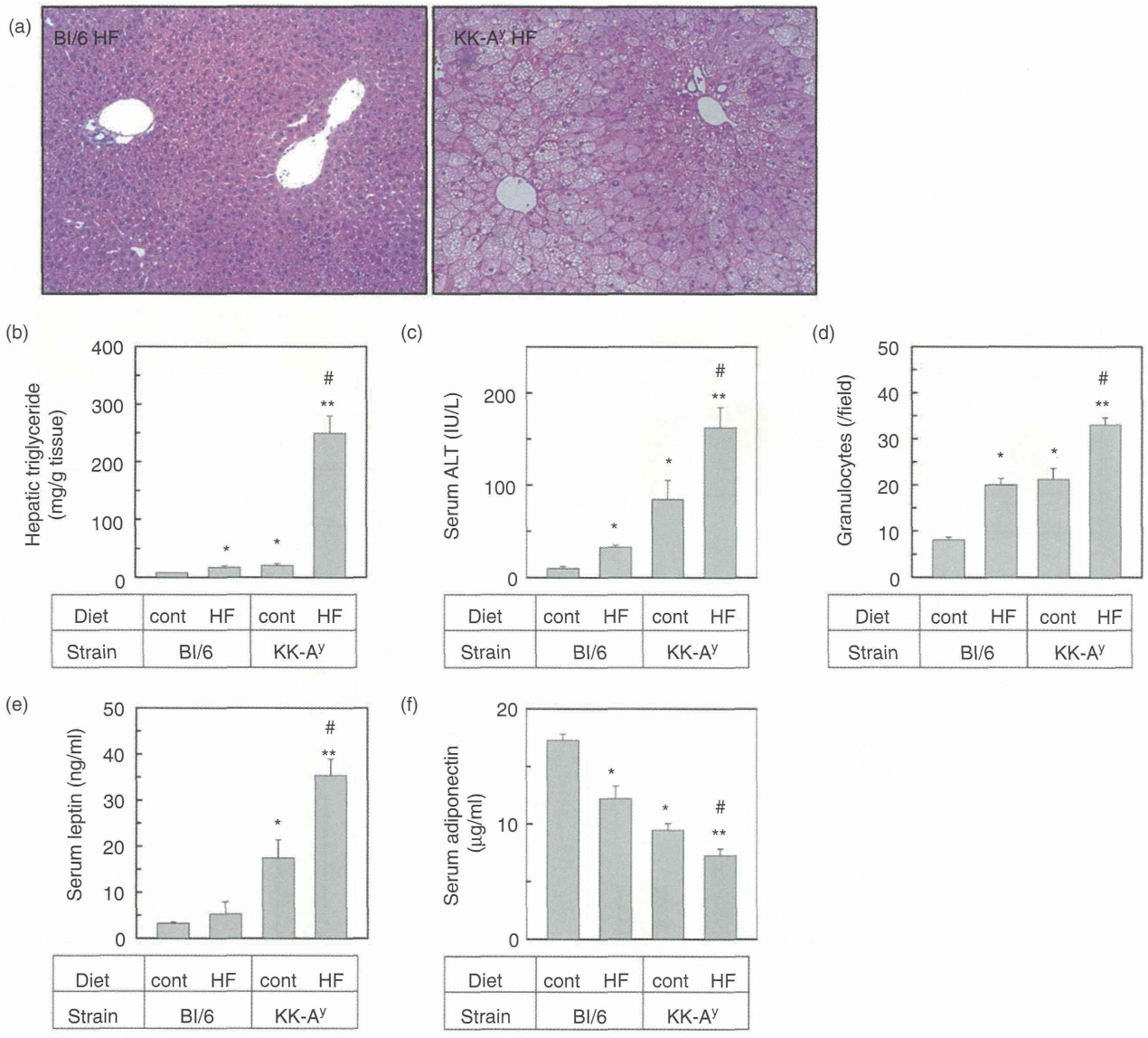

Figure 2 HF diet induces severe steatohepatitis in KK-A^y mice. Both C57Bl/6 and KK-A^y mice were fed a HF or control (cont) diet for 4 weeks. Representative photomicrographs of liver histology from HF diet-fed C57Bl/6 mice (a; left panel) and KK-A^y mice (a; right panel) are shown (hematoxylin–eosin, original magnification ×100). Hepatic triglyceride contents (b) and serum ALT levels (c) were measured, and granulocytes in hepatic lobules were counted using esterase staining (d). Serum levels of leptin (e) and adiponectin (f) were measured by enzyme-linked immunoassay. Data represent mean ± SEM ($n = 5$, $^*P < 0.05$ vs Bl/6 controls, $^{**}P < 0.05$ vs HF-fed Bl/6, $\#P < 0.05$ vs KK-A^y controls, by ANOVA on ranks and Student–Newman–Keuls post-hoc test). ALT, alanine aminotransferase; GalCer, α-galactosylceramide; HF, high fat; IFN, interferon; IL, interleukin; NKT cells, natural killer T cells; SEM, standard error of the mean.

tively, alteration in hepatic NKT cells most likely exerts a variety of actions in the pathogenesis and progression of steatohepatitis.

Our observations are in part coincident with the previous report that hepatic NKT cells are depleted in *ob/ob* mice, which develop severe hepatic steatosis spontaneously. However, with respect to expression profile of adipokines, *ob/ob* mice completely lack functional leptin expression, whereas KK-A^y mice present remarkable hyperleptinemia (Fig. 2e) as observed in common obese